Talanta 188 (2018) 685–690

Contents lists available at ScienceDirect

Talanta

journal homepage: www.elsevier.com/locate/talanta

DNA-fueled target recycling-induced two-leg DNA walker for amplified electrochemical detection of nucleic acid

Kun Wang[a], Min Feng[b], Meng-Qi He[a], Fu-Heng Zhai[a], Yu Dai[a], Rong-Huan He[a,*], Yong-Liang Yu[a,*]

[a] Department of Chemistry, College of Sciences, Northeastern University, Shenyang 110819, China
[b] The first Affiliated Hospital of Dalian Medical University, Dalian 116011, China

ARTICLE INFO

Keywords:
Entropy-driven amplification
DNA walker
Cascade amplification
DNAzyme motor
Biosensor

ABSTRACT

Taking advantage of the homogeneous and heterogeneous electrochemical biosensors, a simple, sensitive, and selective electrochemical biosensor is constructed by combining entropy-driven amplification (EDA) with DNA walker. This electrochemical biosensor realizes the biorecognition and EDA operation in homogeneous solution, which is beneficial to improve the recognition and amplification efficiency. A two-leg DNA walker generated by EDA can walk on the surface of gold electrode for cleaving the immobilized substrate DNA and releasing the electroactive labels, giving rise to a significant decrease of the electrochemical signal. The immobilization of the electroactive labels ensures the reproducibility and reliability of the biosensor. The present cascade amplification assay can be applied to detect target DNA with a detection limit of 0.29 fM, and base mutations can be easily distinguished. Moreover, the proposed electrochemical biosensor shows a satisfactory performance for the detection of target DNA in human serum. Thus, the novel electrochemical biosensor holds promising potential for a future application in disease diagnosis.

1. Introduction

The amplified biosensors have drawn gradual attention over the past decade for the application in disease diagnosis [1–3], environmental monitoring [4,5], and food security [6–8]. Up until now, numerous amplified biosensors have been reported, including fluorescence [9,10], electrochemical [11,12], surface enhancement Raman [13,14], photoelectric [15,16], and colorimetric aptasensors [17–20]. Among these approaches, electrochemical biosensors have significant advantages, such as high sensitivity, simple instrumentation, and signal stability [21,22]. Hence, electrochemical biosensors attract widespread attentions, and many electrochemical biosensors are developed. To improve the sensitivity of electrochemical biosensors, many signal amplification strategies are constructed on the surface of electrode, such as rolling circle amplifications (RCA) [23,24], nuclease-assisted target recycling, catalytic hairpin assembly (CHA) [25,26], and hybridization chain reaction (HCR) [27,28]. Despite the development of those strategies, they also encounter some weaknesses. First, the environmental interference makes the nuclease-assisted target recycling strategy difficult to apply in complex biosystems [29]. The conventional enzyme-free based hairpin-assemblies, such as CHA and HCR, also have some issues. The temperature, pH, and biomolecules may lead to circuit leakage, giving rise to relatively false-positive signals and high background [30]. Therefore, the exploration of amplification strategy with both favorable performance and reliability will potentially promote the development of electrochemical biosensors.

Recently, an entropy-driven amplification (EDA) system has drawn attention as a milestone report in the DNA amplification circuits [31,32]. As a hairpin- and enzyme-free amplification strategy, the EDA can overcome the weakness of CHA and HCR. Inspired by the novel design, Xiang's group proposed an electrochemical biosensor for electronic detection of microRNA [33]. However, those heterogeneous biosensors suffer from the complex interface operation and washing procedures, which increase the assay time and influence the reproducibility of biosensors. Moreover, the amplification efficiency and biorecognition may be influenced by the electrode surface. The conventional homogeneous electrochemical biosensors mostly operate based on the aggregation or diffusion of electroactive labels, which may influence the reproducibility and reliability of biosensors [34,35]. Thus, it is still a challenge to fabricate an electrochemical biosensor with the features of specificity, sensitivity, reliability and simplicity. Taking into account the strengths and weaknesses of homogeneous and heterogeneous electrochemical biosensors, the construction of a novel biosensor with both heterogeneous interface and homogeneous solution may offer a way to approach the challenge. In other words, the biorecognition and the amplification reaction should occur in homogeneous

* Corresponding authors.
E-mail addresses: herh@mail.neu.edu.cn (R.-H. He), yuyl@mail.neu.edu.cn (Y.-L. Yu).

https://doi.org/10.1016/j.talanta.2018.06.049
Received 15 May 2018; Received in revised form 11 June 2018; Accepted 13 June 2018

solution to guarantee the amplification efficiency and biorecognition. Meanwhile, the electroactive labels are immobilized on the surface of electrode to make sure the reproducibility and reliability of the biosensor [36].

Recently, the cascade amplification strategies have been well developed for constructing the amplification biosensors [37,38]. The key operation for those strategies relies on the integration of different amplification circuitries [39]. Inspired by the concept of the cascade amplification strategies, herein, a novel electrochemical biosensor is constructed by combination of the EDA and DNA walker. In this strategy, the biorecognition and EDA are conducted in homogeneous solution, which is beneficial to improve the recognition and amplification efficiency. After the EDA, a two-leg DNA walker is generated to walk on the surface of electrode. During the walking process, the substrate DNA is cleaved and the immobilized electroactive labels are released, resulting in a significant decrease of the electrochemical signal. The immobilization of the electroactive labels ensures the reproducibility and reliability of the biosensor. Moreover, the DNA walker makes it possible to realize the sensitive detection and minimize the operational difficulty. The present cascade amplification assay can be applied for the detection of target DNA with a detection limit of 0.29 fM, and base mutations can be easily distinguished. Thus, the novel electrochemical biosensor holds great potential for point-of-care applications.

2. Experimental

2.1. Chemicals and materials

The tris (2-carboxyethyl) phosphine (TCEP), 4S red plus nucleic acid stain, glycerol gel loading buffer, and HPLC-purified DNA oligonucleotides were purchased from Shanghai Sangon Biotechnology Co (Shanghai, China). The 6-mercaptohexanol (MCH) was purchased from Sigma-Aldrich (St. Louis, MO, U.S.A.). The DNA was dissolved in 25 mM Tris-HCl buffer containing 200 mM NaCl (pH 7.4), and quantified by measuring UV–visible absorption spectroscopy (Varian, USA) at 260 nm. The DNA sequences are listed in Table S1. All other chemicals not mentioned here were analytical reagent grade and used as received. Milli-Q ultrapure water (18.2 MΩ) was used throughout the experiment.

2.2. Modification of gold electrode

The gold electrode (GE) (3 mm diameter) was pretreated according to the previous procedures [35]. The pretreated GE was immersed into the 25 mM Tris-HCl buffer (200 mM NaCl, 10 mM TCEP, pH 7.4) containing 1 μM substrate DNA (SD) for 12 h at room temperature. After washing with phosphate buffer solution (PBS) and drying with nitrogen, the GE was immersed into 1 mM MCH for 30 min to remove the nonspecific adsorption.

2.3. Cascaded isothermal amplification strategy

The mixture of template stand (TS), assistant probe (AP), and block probe (BP) was heated at 90 °C for 10 min, and then allowed to cool down to room temperature to form three-strand complex. Upon optimizing conditions, various concentrations of target DNA (TD) were added in 5 nM three-strand complex containing 10 nM fuel strand (FS) to maintain for 1 h. Afterward, the SD modified GE were immersed into the mixture, and 1 mM Pb^{2+} was added to initiate the cleavage reaction. After incubation at 37 °C for 80 min, the GE was washed with buffer to remove any remaining physi-sorbed methylene or Pb^{2+}. For human serum samples, the human serum was 50-fold diluted with buffer, and then various concentrations of TD were added to the diluted serum sample and detected with the same procedure. Electrochemical measurements were performed by using CHI660C electrochemistry workstation (Co. Chenhua, China) with the modified GE as working electrode, Ag/AgCl electrode as reference electrode, and platinum electrode as counter electrode. The electrochemical impedance spectroscopy (EIS) was recorded in 5 mM $Fe(CN)_6^{3-/4-}$ solution containing 0.1 M KCl. The square wave voltammetry (SWV) was carried out in Tris-HCl buffer with potential window from 0 to 0.45 V.

2.4. Native polyacrylamide gel electrophoresis

Polyacrylamide gel (15%) was prepared with 1 × Tris-borate-EDTA buffer (89 mM Tris, 89 mM boric acid, 2 mM EDTA, pH 8.3). Each sample was prepared with 1 × Tris-borate-EDTA buffer containing 12 mM Mg^{2+}, and the concentration of each DNA strand was 1 μM. 10 μL of each sample was mixed with 1.5 μL of 6 × glycerol gel loading buffer before loading into the gel. The gel electrophoresis was conducted under a constant voltage of 100 V over a period of ~ 2.5 h. After 4 S Red Plus staining, photographs were taken under UV light by using a fluorescence imaging system (Life Science Research Products and System Engineering, China).

3. Results and discussion

3.1. Principle of cascade amplification strategy

The cascade amplification strategy is constructed by the combination of EDA and DNA walker, as illustrated in Scheme 1. The EDA system consists of four strands, i.e., template stand (TS), assistant probe (AP), block probe (BP), and fuel strand (FS). The three-strand complex is prepared by the hybridization of TS, AP, and BP. TS and FS are engineered with a protruding metal-depended DNAzyme tail sequence, which is designed to be complementary to the substrate strand (SD) with a predesigned low melting temperature. In the presence of target DNA (TD), TD could hybridize with the toehold (yellow region) of TS to form an intermediate four-strand structure. Then, AP is dissociated from the four-strand structure, because the complementary fragment between AP and TS is too short to keep AP attached. After the dissociation of AP, the red region is exposed to facilitate the binding of FS to form a four-strand structure. As a result, FS is completely hybridized with TS by branch migration, giving rise to the release of TD and BP. The released TD would initiate a new successive recycling process. The product of TS/FS complex brings the DNAzyme sequence into close proximity with the increase of their local concentration, making the DNAzyme hybridize with the surface-tethered SD. Then, the TS/FS complex could autonomously walk on the surface of GE, which is fueled by DNAzyme-catalyzed substrate cleavage. Scheme 1 depicts the concept of the DNAzyme walker. For the purpose of electrochemical detection, SD is labelled with methylene blue (MB). When the DNAzyme walker is activated by the EDA, the DNAzyme cleaves the SD into two fragments with the help of Pb^{2+}, resulting in the release of MB-labelled segment and the decrease of the electrochemical signal. After cleavage, the DNAzyme would quickly hybridize to the neighboring SD by strand-displacement reaction. Thus, the cleavage of SD ensures the DNA walker autonomously walks on the surface of GE and continuously release the redox labels, leading to a significant signal amplification. TD is detected by monitoring the amplified electrochemistry signal. In the absence of TD, the EDA is blocked by AP and BP, without the hybridization of FS and TS. The DNAzyme sequence, whether in TS or FS, could not associate with SD, because the complementary fragment is too short to promote an effective annealing.

3.2. Feasibility and optimizations

To test the feasibility of the cascade amplification strategy, the electrochemical signals in the presence of various components are measured by SWV. As shown in Fig. S1, a maximal electrochemical response of MB (curve a) is observed for the solution containing three-strand complex, because the complementary fragment of TS/SD is too

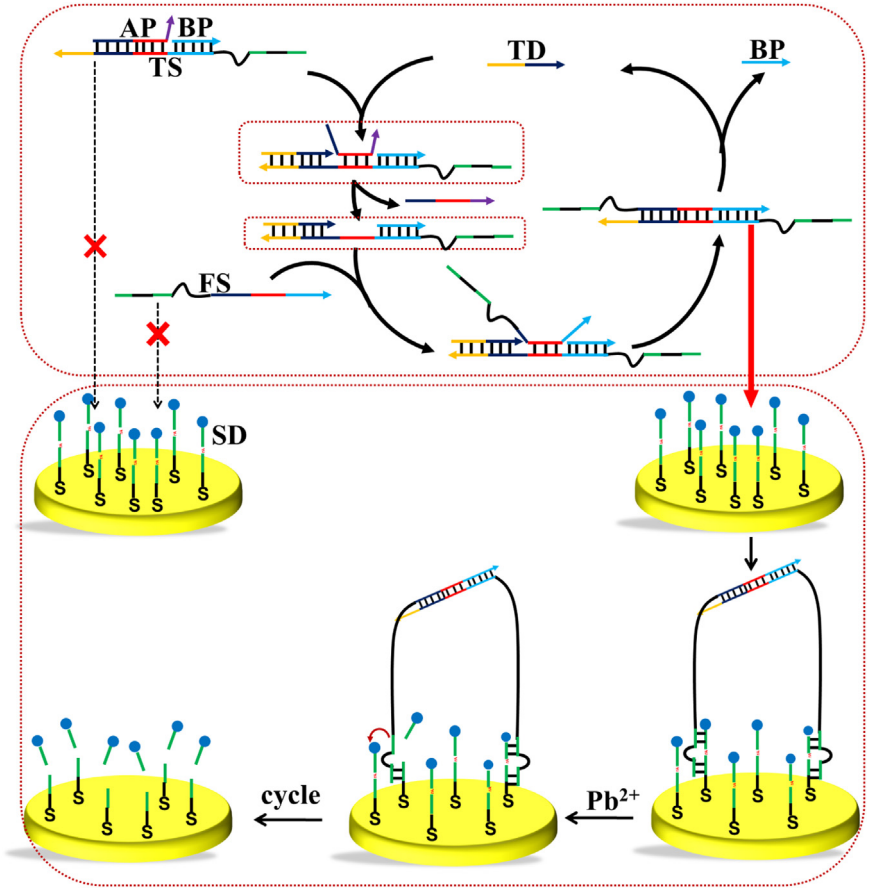

Scheme 1. Schematic illustration of DNA-fueled target recycling-induced two-leg DNA walker for amplified electrochemical detection of the nucleic acid.

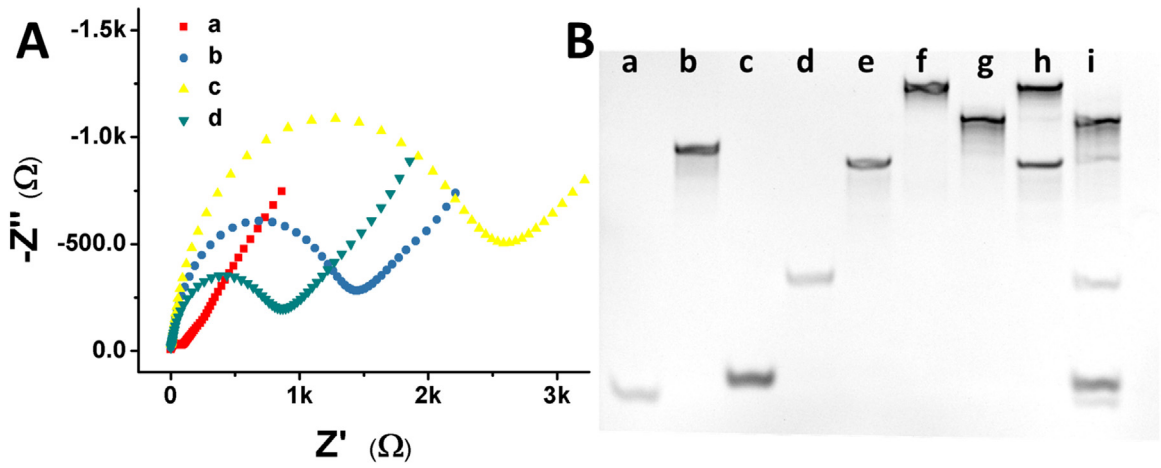

Fig. 1. (A) Electrochemical impedance spectra (EIS) of gold electrode (GE) after each step of surface modification: (a) bare GE; (b) SD modified GE; (c) SD modified GE incubated with 5 nM three-strand complex (TS/AP/BP), 10 nM FS, and 2 pM TD for 1 h; (d) further incubated with 1 mM Pb^{2+}. (B) Polyacrylamide gel electrophoresis (PAGE) analysis of EDA: (a) TD; (b) TS; (c) BP; (d) AP; (e) FS; (f) TS/AP/BP; (g) TS/FS; (h) TS/AP/BP/FS; (i) TS/AP/BP/FS /TD.

short to promote an effective annealing. Upon the addition of the FS, the electrochemical signal exhibits a negligible change, because the EDA is blocked by AP and BP (curve b). When the TD is added into the solution, the visible electrochemical signal change of MB (curve c) is obtained. It is because that the product of EDA (TS/FS complex) brings the DNAzyme sequence into close proximity with the increase of their local concentrations, making the DNAzyme hybridize with the surface-tethered SD. The electrochemical signal dramatically decreases after incubation with Pb^{2+}, indicating the cleavage of SD (curve d). The electrochemistry impedance spectroscopy (EIS) is also employed to characterize the surface of GE. As shown in Fig. 1A, the bare GE exhibits an almost straight line, indicating that its charge transfer resistance (*Rct*) is very low. The *Rct* increases significantly after conjugation of SD, because the negatively charged DNA on the surface of GE blocks the electron transfer. The *Rct* further increases after incubation of TD, indicating that the hybridization between TS/FS complex and SD occurs. After incubation of Pb^{2+}, the *Rct* dramatically decreases, thereby demonstrating the cleavage of SD and the release of DNA fragments. To further confirm the EDA, polyacrylamide gel electrophoresis (PAGE) is employed to verify the strand displacement reaction in the EDA. As

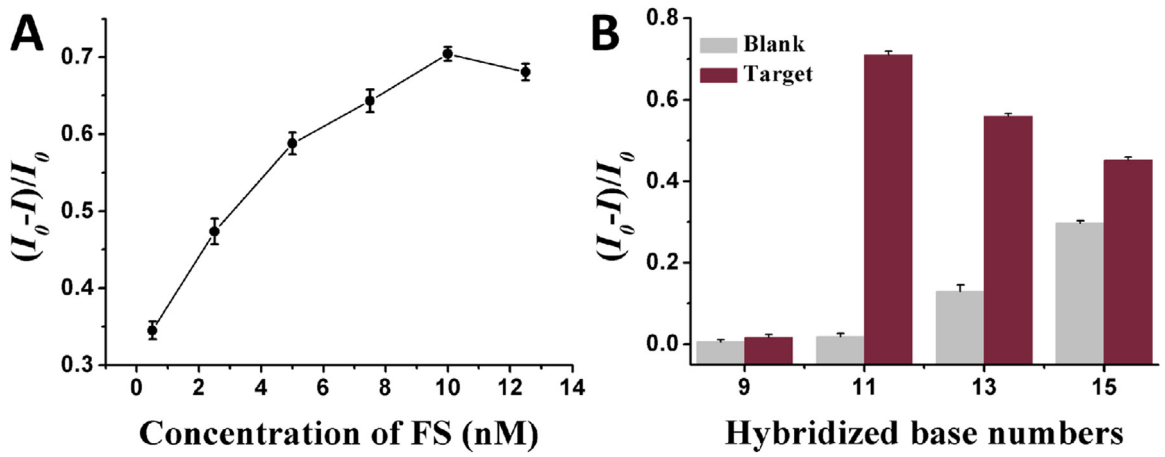

Fig. 2. (A) Dependence of the ratio of $(I_0\text{-}I)/I_0$ on FS concentration in the presence of 2 pM target DNA; (B) Current changes at different base pairing sequences of DNAzyme/substrate.

shown in Fig. 1B, the line a, b, c, d, e, f, and g correspond to strand TD, TS, BP, AP, FS, TS/AP/BP, and TS/FS, respectively. In the lane h, the presence of two strong bands corresponding to the complexes of TS/AP/BP and FS indicates that the EDA is silent in the absence of TD. In the presence of TD, almost all TS/AP/BP complexes are converted to TS/FS with obvious bands of AP and BP (lane i). The results of PAGE demonstrate the feasibility of EDA.

In order to ensure the performance of the biosensor, the influence of FS concentration is examined and optimized. The concentration of FS could influence the amplification efficiency of EDA and the detection sensitivity. As shown in Fig. 2A, the ratio of $(I_0\text{-}I)/I_0$ (I_0 and I represent the peak current in the absence and presence of TD) increases with the increase in concentration of FS, and reaches the maximum at 10 nM. Excess FS concentration, e.g., more than 10 nM, would restrain the catalytic reaction. Thus, 10 nM FS is employed for the EDA. To ensure the high mobility of DNA walker and low background signal, DNAzyme and substrate are designed with different numbers of base pairs. In this strategy, a short hybrid domain between DNAzyme and substrate could significantly reduce the nonspecific cleavage, resulting in a low background signal. However, too short binding domain is not beneficial to form a stable complex between substrate and DNAzyme, which may fail to obtain an electrochemical signal change. As shown in Fig. 2B, when the hybridized base number of the DNAzyme/substrate complex is 11, the ratio of $(I_0\text{-}I)/I_0$ is bigger than those at the hybridized base numbers of 9, 13, and 15. Therefore, the DNAzyme with 11 base pairs complementary to the substrate is chosen for the ensuing experiment. In order to gain the maximal signal response and guarantee the cleavage efficiency of SD, the immobilization concentration of SD is optimized. As shown in Fig. S2, the ratio of $(I_0\text{-}I)/I_0$ increases with the increased SD concentration up to 1 μM, and then decreases as further increasing the SD concentration due to the electrostatic repulsion and steric hindrances. Thus, the maximal signal change could be obtained at the SD concentration of 1 μM.

Further investigations on the influences of Pb^{2+} concentration, incubation time, and temperature are performed. The concentration of Pb^{2+} could directly influence the catalytic activity of DNAzyme. As shown in Fig. 3A, the cascade amplification biosensor operates reliably in the presence of 1–2 mM Pb^{2+}. Therefore, Pb^{2+} concentration of 1 mM is recommended for the determination of TD in the following experiment. As shown in Fig. 3B, the progress curve of the sensing system is also recorded by using electrochemical monitor. In the absence of TD, the signal response is almost stable. Upon the addition of TD, the electrochemical response increases along with time, and reaches the saturation at 80 min. Therefore, 80 min is selected as the optimal incubation time to ensure the best analysis capability.

3.3. Analytical performance of the electrochemical biosensor

Under the optimal operating conditions, the analytical performance of the biosensor is evaluated by detecting various concentrations of TD. As shown in Fig. 4A, the SWV curve shows a sharp reduction peak at − 0.244 V, and the SWV peak current dynamically decreases with increasing the TD concentration. As shown in Fig. 4B, a good linear relationship is observed between the ratio of $(I_0\text{-}I)/I_0$ and the concentration of TD within a range from 0.3 to 500 fM. The regression equation is $(I_0\text{-}I)/I_0 = 0.135–0.21C_{TD}$ (C_{TD} represents the concentration of TD). A detection limit of 0.29 fM is obtained based on the calculation of 3σ/slope. Such a detection limit is comparable to the previously reported biosensors for DNA detection (Table S2). The ultrahigh sensitivity may be attributed to three aspects. First, the target initiated EDA could produce abundant DNA walkers. Second, the DNAzyme on the tail sequence of the DNA walker would autonomously cleave the substrate on the surface of GE, which is the fundamental guarantee of sensitivity. Moreover, the surface-tethered DNA walker can obtain a certain extent signal change even without the cleavage of the substrate, because the duplex structure of DNAzyme/substrate makes the MB far away from the GE. The linear response range and LOD obtained by the present electrochemical biosensor are much better than those reported in our previous electrochemical biosensor based on DNA nanomachine modified on the surface of GE [40], which could be attributed to the unique design by combining the advantages of homogeneous and heterogeneous electrochemical biosensors.

3.4. Selectivity and real sample analysis of the electrochemical biosensor towards target DNA

The selectivity of the present electrochemical biosensor is investigated by monitoring the electrochemical response towards various mutants of TD. As illustrated in Fig. 5A, the single-base mismatched mutants could only result in 10.7% (M1a) and 18.4% (M1b) of the peak current change ratio to TD, while the two-base and three-base mismatched mutants could result in lower peak current change ratios, indicating the remarkable specificity of the electrochemical biosensor for DNA detection. The high selectivity obtained is attributed to the specificity of EDA and the advantage of biorecognition in homogeneous solutions.

In order to investigate the applicability of the electrochemical biosensor in real biological samples, the target DNA is detected in the 50-fold diluted healthy human serum by using the same procedure. As shown in Fig. 5B, the target DNA could cause a significant electrochemical signal change in serum. Notably, the electrochemical signal of

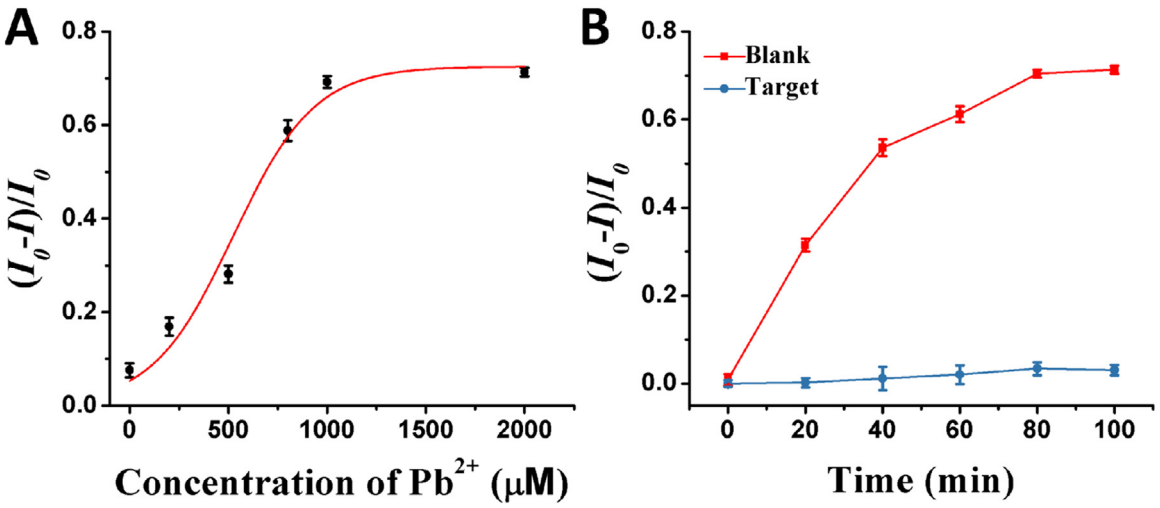

Fig. 3. Effect of Pb^{2+} concentration on the detection of target DNA; (B) Typical progress curve of the DNA nanomachine.

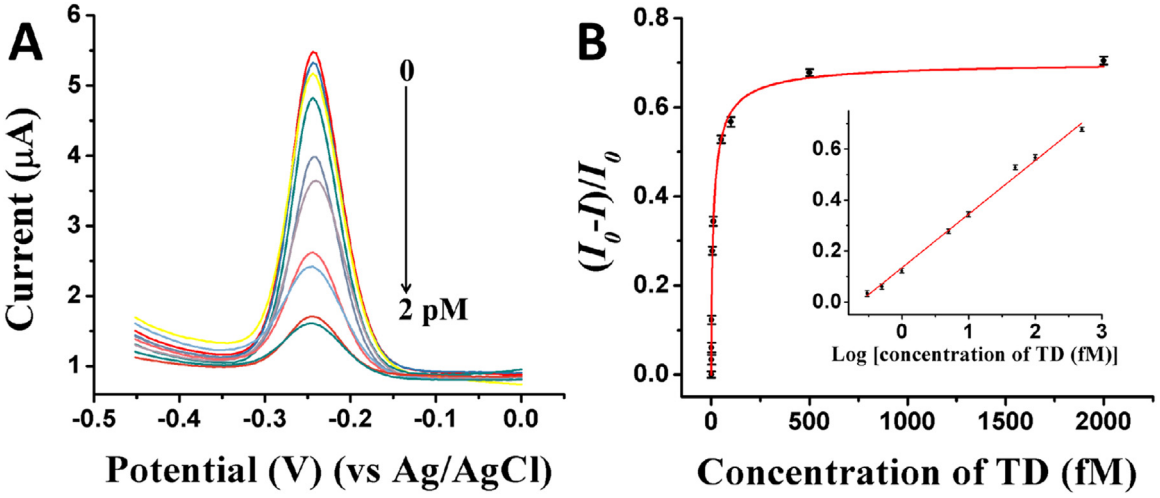

Fig. 4. (A) SWV responses corresponding to various concentrations of target DNA ranging from 0 to 2 pM; (B) The peak current change ratio in the presence of various concentrations of target DNA. Inset: calibration curve of peak current change ratio versus target DNA concentration.

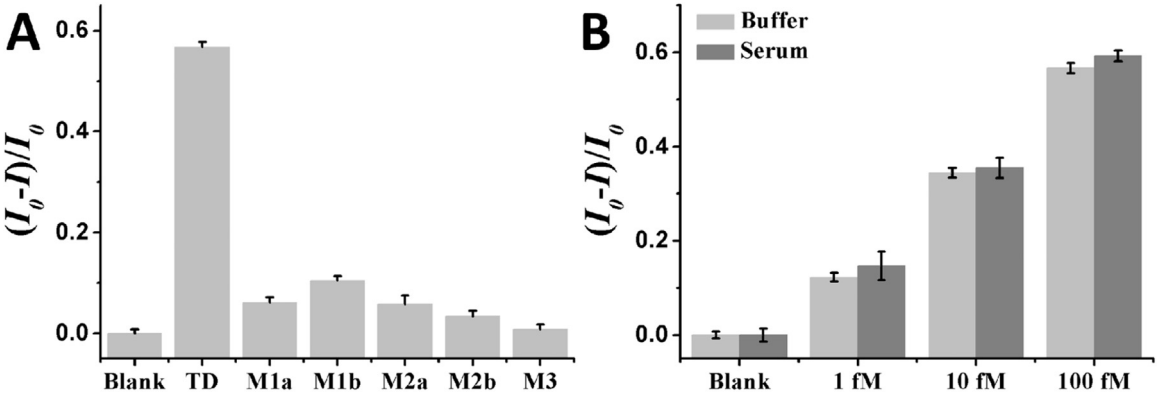

Fig. 5. (A) The peak current change ratio in the presence of target DNA (100 fM) and mutants (2 pM) including M1a, M1b, M2a, M2b and M3; (B) Results obtained from the buffer solution and the diluted serum samples spiked with different concentrations of target DNA. The same reaction mixtures without target DNA are used as controls.

the target DNA obtained from serum is close to that obtained from buffer solution. The results indicate that the present electrochemical biosensor holds great potential for a future application in clinical diagnoses.

4. Conclusions

In this work, a novel DNA nanomachine is proposed for the development of sensitive, selective, and reliable electrochemical biosensor.

EDA and DNA walker are operated in homogeneous solution and heterogeneous interface, respectively. The target DNA triggers the EDA to generate abundant two-leg DNA walkers in the homogeneous solution, which make sure the recognition and amplification efficiency. The cleavage of DNAzyme powers the walking process of two-leg DNA walkers on the surface of GE. Massive substrate DNAs are cleaved and the immobilized electroactive probes are released from GE, which is beneficial for the reproducibility and reliability of the biosensor. Taking advantage of the homogeneous and heterogeneous electrochemical biosensors, the developed biosensor presents a competitive detection limit of 0.29 fM, and single base mismatches are easily distinguished by the reported strategy. Moreover, it can be applied for the quantitative detection of DNA in human serum samples, which shows potential application in bioanalysis and clinical diagnosis.

Acknowledgements

This work is financially supported by the National Natural Science Foundation of China (51572044, 21475018), and the Fundamental Research Funds for the Central Universities (N160504010, N170507001).

Appendix A. Supplementary material

Supplementary data associated with this article can be found in the online version at http://dx.doi.org/10.1016/j.talanta.2018.06.049.

References

[1] K. Zhang, L. Yang, F. Lu, X. Wu, J.-J. Zhu, A universal upconversion sensing platform for the sensitive detection of tumour-related ncRNA through an Exo III-assisted cycling amplification strategy, Small 14 (2018) 1703858.
[2] K. Wang, J.-T. Ren, D.-Q. Fan, Y.-Q. Liu, E.-K. Wang, Integration of graphene oxide and DNA as a universal platform for multiple arithmetic logic units, Chem. Commun. 50 (2014) 14390–14393.
[3] X.-D. Lin, Y.-Q. Liu, Z.-H. Tao, J.-T. Gao, J.-K. Deng, J.-J. Yin, S. Wang, Nanozyme-based bio-barcode assay for high sensitive and logic-controlled specific detection of multiple DNAs, Biosens. Bioelectron. 94 (2017) 471–477.
[4] M.-Q. He, K. Wang, J. Wang, Y.-L. Yu, R.-H. He, A sensitive aptasensor based on molybdenum carbide nanotubes and label-free aptamer for detection of bisphenol A, Anal. Bioanal. Chem. 40 (2017) 1797–1803.
[5] C.-P. Huang, X.-Y. Fan, Q.-M. Yuan, X.-F. Zhang, X.-D. Hou, P. Wu, Colorimetric determination of uranyl (UO_2^{2+}) in seawater via DNAzyme-modulated photosensitization, Talanta 185 (2018) 258–263.
[6] X. Liu, N. Xu, P. Gai, F. Li, Triplex DNA formation-mediated strand displacement reaction for highly sensitive fluorescent detection of melamine, Talanta 185 (2018) 352–358.
[7] X.-D. Lin, Y.-Q. Liu, J.-K. Deng, Y.-L. Lyu, P.-C. Qian, Y.-F. Li, S. Wang, Multiple advanced logic gates made of DNA-Ag nanocluster and the application for intelligent detection of pathogenic bacterial genes, Chem. Sci. 9 (2018) 1774–1781.
[8] H. Hu, J. Zhang, Y. Ding, X. Zhang, K.-L. Xu, X. Hou, P. Wu, Modulation of the singlet oxygen generation from the double strand DNA-SYBR Green I complex mediated by T-melamine-T mismatch for visual detection of melamine, Anal. Chem. 89 (2017) 5101–5106.
[9] J.-B. Chen, A. Zuehlke, B. Deng, H.-Y. Peng, X.-D. Hou, H.-Q. Zhang, A target-triggered DNAzyme motor enabling homogeneous, amplified detection of proteins, Anal. Chem. 89 (2018) 12888–12895.
[10] K. Wang, M.-Q. He, F.-H. Zhai, R.-H. He, Y.-L. Yu, A label-free and enzyme-free ratiometric fluorescence biosensor for sensitive detection of carcinoembryonic antigen based on target-aptamer complex recycling amplification, Sens. Actuators B-Chem. 253 (2017) 893–899.
[11] X. Li, J. Li, C. Zhu, X. Zhang, J. Chen, A new electrochemical immunoassay for prion protein based on hybridization chain reaction with hemin/G-quadruplex DNAzyme, Talanta 182 (2018) 292–298.
[12] H. Wang, S. Zhang, S. Li, J. Qu, Electrochemical sensor based on palladium-reduced graphene oxide modified with gold nanoparticles for simultaneous determination of acetaminophen and 4-aminophenol, Talanta 178 (2018) 188–194.
[13] Y. Si, Y. Bai, X. Qin, J. Li, W. Zhong, Z. Xiao, J. Li, Y. Yin, Alkyne–DNA-functionalized alloyed Au/Ag nanospheres for ratiometric surface-enhanced Raman scattering imaging assay of endonuclease activity in live cells, Anal. Chem. 90 (2018) 3898–3905.
[14] J.-Y. Kim, Z.-C. Zeng, L. Xiao, Z.D. Schultz, Elucidating protein/ligand recognition with combined surface plasmon resonance and surface enhanced Raman spectroscopy, Anal. Chem. 89 (2017) 13074–13081.
[15] J. Li, J. Wang, Z. Dai, H. Li, Disordered photonics coupled with embedded nano-Au plasmonics inducing efficient photocurrent enhancement, Talanta 176 (2018) 428–436.
[16] Y.C. Zhu, N. Zhang, Y.F. Ruan, W.-W. Zhao, J.-J. Xu, H.-Y. Chen, Alkaline phosphatase tagged antibodies on gold nanoparticles/TiO_2 nanotubes electrode: a plasmonic strategy for label-free and amplified photoelectrochemical immunoassay, Anal. Chem. 88 (2016) 5626–5630.
[17] Y.-H. Guo, K.-L. Yang, J.-C. Sun, J. Wu, H.-X. Ju, A pH-responsive colorimetric strategy for DNA detection by acetylcholinesterase catalyzed hydrolysis and cascade amplification, Biosens. Bioelectron. 94 (2018) 651–656.
[18] Z.-F. Shen, F. Li, Y.-F. Jiang, C. Chen, H. Xu, C.-C. Li, Z. Yang, Z.-S. Wu, Palindromic molecule beacon-based cascade amplification for colorimetric detection of cancer genes, Anal. Chem. 90 (2018) 3335–3340.
[19] K. Wang, D.-Q. Fan, Y.-Q. Liu, E.-K. Wang, Highly sensitive and specific colorimetric detection of cancer cells via dual-aptamer target binding strategy, Biosens. Bioelectron. 73 (2015) 1–6.
[20] H. Xia, J. Hu, J. Tang, K.-L. Xu, X.-D. Hou, P. Wu, A RGB-type quantum dot-based sensor array for sensitive visual detection of trace formaldehyde in air, Sci. Rep. 6 (2016) 36794.
[21] H. Qi, S. Yue, S. Bi, C. Ding, W. Song, Isothermal exponential amplification techniques: from basic principles to applications in electrochemical biosensors, Biosens. Bioelectron. 110 (2018) 207–217.
[22] Y. Chang, Y. Zhuo, Y. Chai, R. Yuan, Host-guest recognition-assisted electrochemical release: its reusable sensing application based on DNA cross configuration-fueled target cycling and strand displacement reaction amplification, Anal. Chem. 89 (2017) 8266–8272.
[23] J. Huang, X.-Y. Li, Y.-C. Du, L.-N. Zhang, K.-K. Liu, L.-N. Zhu, D.-M. Kong, Sensitive fluorescent detection of DNA methyltransferase using nicking endonuclease-mediated multiple primers-like rolling circle amplification, Biosens. Bioelectron. 91 (2018) 417–423.
[24] Y. Luo, X. Yan, Y. Huang, R. Wen, Z. Li, L. Yang, C.-J. Yang, Q. Wang, ICP-MS-based multiplex and ultrasensitive assay of viruses with lanthanide-coded biospecific tagging and amplification strategies, Anal. Chem. 85 (2013) 9428–9432.
[25] Y. Gu, J. Song, M.-X. Li, T.-T. Zhang, W. Zhao, J.-J. Xu, M. Liu, H.-Y. Chen, Ultrasensitive microRNA assay via surface plasmon resonance responses of Au@Ag nanorods etching, Anal. Chem. 89 (2017) 10585–10591.
[26] Y. Jiang, B. Li, J.N. Milligan, S. Bhadra, A.D. Ellington, Real-time detection of isothermal amplification reactions with thermostable catalytic hairpin assembly, J. Am. Chem. Soc. 135 (2013) 7430–7433.
[27] S. Shimron, F. Wang, R. Orbach, I. Willner, Amplified detection of DNA through the enzyme-free autonomous assembly of hemin/G-quadruplex DNAzyme nanowires, Anal. Chem. 84 (2011) 1042–1048.
[28] Z. Wu, G.-Q. Liu, X.-L. Yang, J.-H. Jiang, Electrostatic nucleic acid nanoassembly enables hybridization chain reaction in living cells for ultrasensitive mRNA imaging, J. Am. Chem. Soc. 137 (2015) 6829–6836.
[29] X. Jiang, H. Wang, H. Wang, Y. Zhuo, R. Yuan, Y. Chai, Electrochemiluminescence biosensor based on 3-D DNA nanomachine signal probe powered by protein-aptamer binding complex for ultrasensitive mucin 1 detection, Anal. Chem. 89 (2017) 4280–4286.
[30] Y. Lv, L. Cui, R. Peng, Z. Zhao, L. Qiu, H. Chen, C. Jin, X.-B. Zhang, W. Tan, Entropy beacon: a hairpin-free DNA amplification strategy for efficient detection of nucleic acids, Anal. Chem. 87 (2015) 11714–11720.
[31] S. Ou, T. Xu, X. Liu, X. Yu, R. Li, J. Deng, J. Yuan, Y. Chen, Rapid and ultrasensitive detection of microRNA based on strand displacement amplification-mediated entropy-driven circuit reaction, Sens. Actuators B-Chem. 255 (2018) 3057–3063.
[32] D.Y. Zhang, A.J. Turberfield, B. Yurke, E. Winfree, Engineering entropy-driven reactions and networks catalyzed by DNA, Science 318 (2007) 1121–1125.
[33] K. Shi, B. Dou, C. Yang, Y. Chai, R. Yuan, Y. Xiang, DNA-fueled molecular machine enables enzyme-free target recycling amplification for electronic detection of microRNA from cancer cells with highly minimized background noise, Anal. Chem. 87 (2015) 8578–8583.
[34] L. Ge, W. Wang, X. Sun, T. Hou, F. Li, Affinity-mediated homogeneous electrochemical aptasensor on a graphene platform for ultrasensitive biomolecule detection via exonuclease-assisted target-analog recycling amplification, Anal. Chem. 88 (2016) 2212–2219.
[35] C. Li, X. Li, L. Wei, M. Liu, Y. Chen, G. Li, Simple electrochemical sensing of attomolar proteins using fabricated complexes with enhanced surface binding avidity, Chem. Sci. 6 (2015) 4311–4317.
[36] S. Liu, L. Fang, Y. Wang, L. Wang, Universal dynamic DNA assembly-programmed surface hybridization effect for single-step, reusable, and amplified electrochemical nucleic acid biosensing, Anal. Chem. 89 (2017) 3108–3115.
[37] M.-Q. He, K. Wang, W.-J. Wang, Y.-L. Yu, J.-H. Wang, Smart DNA machine for carcinoembryonic antigen detection by exonuclease III-assisted target recycling and DNA walker cascade amplification, Anal. Chem. 89 (2017) 9292–9298.
[38] Y. Zhao, F. Chen, M. Lin, C. Fan, A methylation-blocked cascade amplification strategy for label-free colorimetric detection of DNA methyltransferase activity, Biosens. Bioelectron. 54 (2014) 565–570.
[39] K. Wang, D. Fan, Y. Liu, S. Dong, Cascaded multiple amplification strategy for ultrasensitive detection of HIV/HCV virus DNA, Biosens. Bioelectron. 87 (2017) 116–121.
[40] K. Wang, M.-Q. He, F.-H. Zhai, J. Wang, R.-H. He, Y.-L. Yu, Autonomous DNA nanomachine based on cascade amplification of strand displacement and DNA walker for detection of multiple DNAs, Biosens. Bioelectron. 105 (2018) 159–165.